

Article

# Fossil Resins—Constraints from Portable and Laboratory Near-infrared Raman Spectrometers

Beata Naglik <sup>1,\*</sup>, Maja Mroczkowska-Szerszeń <sup>2</sup>, Magdalena Dumańska-Słowik <sup>3</sup>,  
Lucyna Natkaniec-Nowak <sup>3</sup>, Przemysław Drzewicz <sup>4</sup>, Paweł Stach <sup>3</sup> and Grażyna Żukowska <sup>5</sup>

<sup>1</sup> Polish Geological Institute-National Research Institute, Upper Silesian Branch, 1 Królowej Jadwigi Str., 41-200 Sosnowiec, Poland

<sup>2</sup> Oil and Gas Institute-National Research Institute, 25A Lubicz Str., 31-503 Krakow, Poland; mroczkowska@inig.pl

<sup>3</sup> Faculty of Geology, Geophysics and Environmental Protection, AGH University of Science and Technology, 30 Mickiewicz Av., 30-059 Krakow, Poland; dumanska@agh.edu.pl (M.D.-S.); natkan@agh.edu.pl (L.N.-N.); ppawel.stachh@gmail.com (P.S.)

<sup>4</sup> Polish Geological Institute-National Research Institute, 4 Rakowiecka Str., 00-975 Warsaw, Poland; pdrz@pgi.gov.pl

<sup>5</sup> Faculty of Chemistry, Warsaw University of Technology, 3 Noakowskiego Str., 00-664 Warsaw, Poland; zosia@ch.pw.edu.pl

\* Correspondence: beata.naglik@op.pl

Received: 6 December 2019; Accepted: 17 January 2020; Published: 25 January 2020



**Abstract:** Comparative studies of fossil resins of various ages, botanical sources, geological environments, and provenience were provided via a handheld portable Near-Infrared (NIR)-Raman spectrometer and benchtop instrument both working with laser line 1064 nm. The recorded Raman spectra of individual fossil resins were found to be sufficiently similar irrespective to the device type applied, i.e., handheld or benchtop. Thus, the portable equipment was found to be a sufficient tool for the preliminary identification of resins based on botanical and geographical origin criteria. The observed height ratio of 1640/1440 cm<sup>-1</sup> Raman bands did not correlate well with the ages of fossil resins. Hence, it may be assumed that geological conditions such as volcanic activity and/or hydrothermal heating are plausible factors accelerating the maturation of resins and cross-linking processes.

**Keywords:** fossil resins; NIR-Raman spectroscopy; 1064 nm laser line; maturation; fossilization; polymerization

## 1. Introduction

Fossil resins are sticky plant secretions that harden on atmospheric exposure over time, and have been found within coal or other sedimentary rocks. They were formed tens of millions of years ago through the diagenetic or catagenetic transformations of plant exudates induced by various geochemical processes. From a chemical point of view, they are water-insoluble complex mixtures of organic compounds such as terpenes, terpenoids and their derivatives [1–5]. Occurring in various worldwide localities, fossil resins are incorporated in geological layers spanning in age from the Triassic to Cenozoic [6,7]. They differ from one deposit to another in terms of physicochemical properties (appearance) as well as the presence of organic and inorganic inclusions. These differences reflect the evolutionary history of the resins from the initial botanical source to the present, fossil form. Besides that, the exudates from the same botanical source sometimes undergo different fossilization processes resulting in the formation of many varieties of fossil resins. Among the huge number of resin types, the succinite (Baltic amber), containing succinic acid, remains the most frequently studied [8–13].

Since the mid-twentieth century, Fourier Transform Infrared Spectroscopy (FT-IR) has become a fundamental method for classification and origin interpretation of fossil resins [14–18]. However, the diagnostic significance of the FT-IR technique became disputable since the characteristic spectral pattern within the diagnostic absorption range of 1250–1150  $\text{cm}^{-1}$  (known as the “Baltic shoulder”) was also observed in samples other than Baltic ambers [19]. Lately, the comprehensive approach to the investigation of fossil resins has become more complex due to the availability of various advanced analytical methods adopted from chemical and physical sciences [17]. Although many instrumental techniques have become successfully employed in fossil resin studies, i.e., scanning electron microscopy with electron dispersive spectroscopy [12,20,21], Raman microspectroscopy [19,22–37], gas chromatography-mass spectrometry (GC-MS) [38,39], Nuclear Magnetic Resonance spectroscopy (NMR) [40–42], thermal analysis [43–45] and microhardness testing [46,47], the unambiguous identification and classification of fossil resins is still a very challenging task. Some doubts regarding fossil resin origin, their botanical affinities, alteration in the geological environment still exist, and some knowledge gaps require explanation, i.e., the fossilization mechanisms pathways. Therefore, the development and the application of various analytical methods in fossil resin investigation together with a geological, palaeogeographical and palaeoclimatic background is crucial for understanding fossilization processes as well as geological and environmental conditions associated with the transformation of resins from plant exudates to present, fossil forms.

Recently, Raman spectroscopy with an excitation wavelength of 1064 nm and using benchtop equipment [22–26,28–30,33,35,37], as well as a portable technique [33] was successfully applied in research of fossil resins. The main advantage of this method over FT-IR was the easy sample preparation and nearly non-destructive character of the measurements [22,36]. Moreover, Raman microspectroscopy is suitable for analysis of the aromatic or unsaturated compounds, characteristic bands such as C=C stretching, having weak intensity in FT-IR and being additionally overlapped by much stronger bands related to the C=O stretching vibrations [36].

The identification of molecular spectral features of resins, which might allow for discrimination between specimens coming from different geographical locations was undertaken by many authors [23,27,28,37]. It has still remained a challenging task since the fossil resins, in the course of their maturation process, are affected by degradation processes to various degrees, which in consequence leads to the resetting of their spectroscopic fingerprints [19]. However, some fossil resins could still be easily recognized using Raman spectroscopy, i.e., Borneo amber [19] or sieburgite [26]. Raman spectroscopy was found to provide information about the chemical structure of the resins, such as the presence of cyclohexane/cyclopentane derivatives, aromatic rings as well as exocyclic  $\text{CH}_2$  and  $\text{CH}_3$  groups [48]. As the process of fossil resins degradation might affect the shape of their Raman spectra [19], Raman spectroscopy has been commonly used for assessments of the maturation degree of fossil resins that, in turn, may be correlated with the age of the specimens [24,25], geological setting of the deposit as well as redox, temperature and pressure conditions during fossilization [25,28]. Additionally, Raman spectroscopy has already been reported as a successful technique for studies of amber-hosted animal inclusions [19], archaeological objects [27,29] as well as differentiation between amber, copal (immature resins) and colophony [34]. In many cases, preliminary gemmological analyses of fossil resins and their quick identification by the spectrometric method might be sufficient for their authenticity confirmation. Further possibilities result from the use of portable, handheld equipment, which could be very useful, especially in field works, out of a laboratory [26]. The applicability and limits of using a portable Raman spectrometer in mineralogical investigations were discussed recently by Jehlička et al. [31,32] who recommended portable Raman instruments for the fast and easy identification of minerals in the field. On the other hand, the unsatisfactory quality of Raman spectra (low resolution, high background noise and limited signal processing capabilities) is the main drawback that should be considered in choosing between application of the portable and laboratory equipment in the research. Jehlička et al. [31,32] performed an investigation using Raman spectrometers with 785 nm excitation laser line that frequently causes fluorescence interferences resulting in poor quality

of obtained spectra of fossil resins. The problems associated with fluorescence of samples could be avoided by using Near-infrared Raman spectroscopy [22,33]. The laboratory Raman spectrometers with 1064 nm laser line have been available for a long time, but portable equipment has been introduced to the market only quite recently.

In our contribution, ten fossil resins (Figure 1) of various age (from Cretaceous to Miocene), worldwide localities (Ethiopia, Russia, Myanmar, Mexico, the Dominican Republic, Borneo, Sumatra), and botanical sources (*Araucariaceae/Pinaceae/Cupressaceae*, *Cupressaceae/Taxodiaceae*, *Hymenaea*, *Dipterocarpus*, *Dipterocarpaceae*) were investigated with both handheld and laboratory equipment using 1064 nm laser line excitation. Based on NIR-Raman spectral characteristics, the resins were grouped to compare their age, botanical and geographical origin as well as environmental and geological conditions occurring during their formation and alteration. Finally, the potential for portable NIR-Raman spectroscopy as a tool for rapid and non-destructive fossil resins identification and classification is discussed in detail.

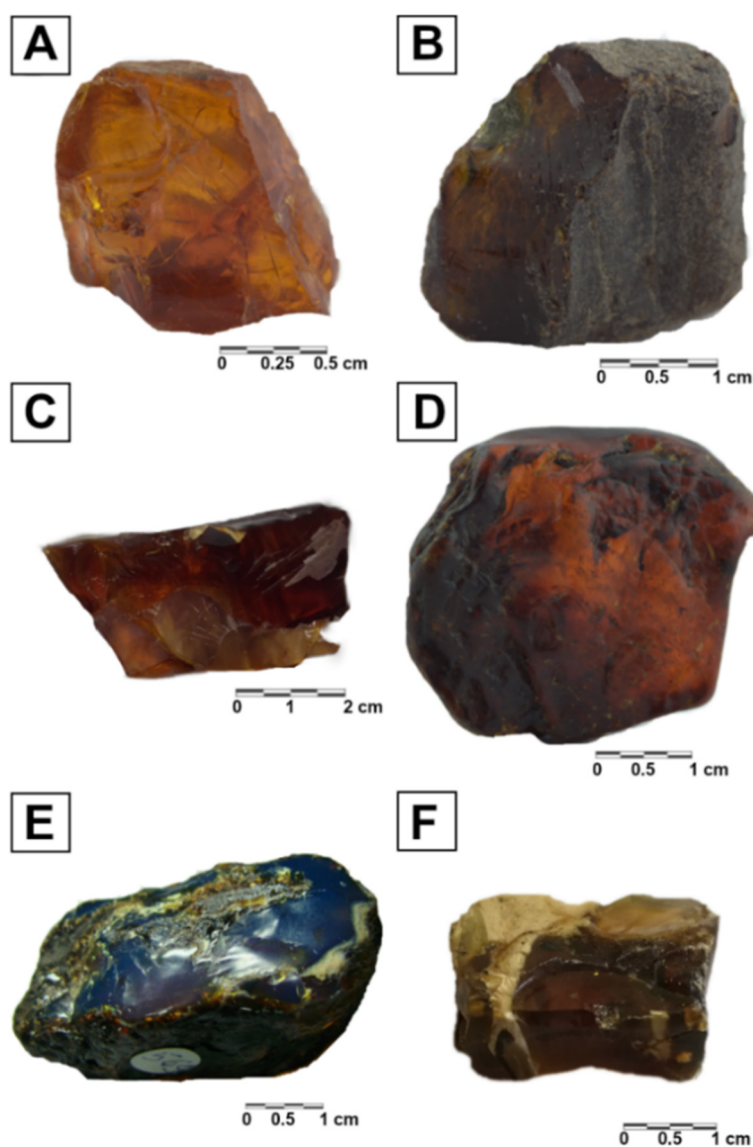
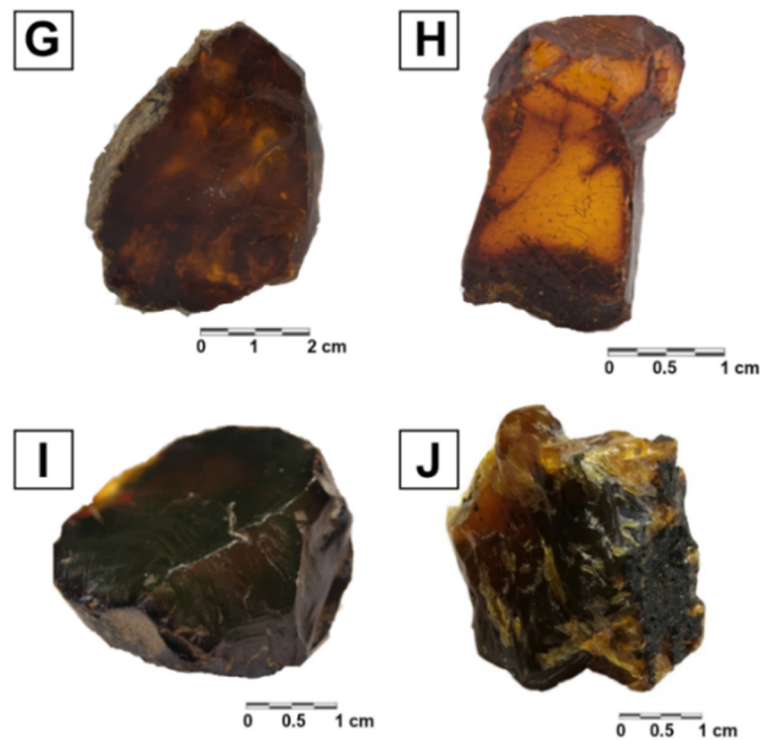


Figure 1. Cont.



**Figure 1.** Macrophotos of fossil resins: (A)—Khatanga, Russia; (B)—Alem Ketema, Ethiopia; (C)—Hukawng valley, Myanmar; (D)—Sakhalin, Russia; (E)—Sumatra (Palembang Province), Indonesia; (F)—Sumatra (Jambi Province), Indonesia; (G)—Chiapas, Mexico; (H)—Santiago de los Caballeros, Dominican Republic; (I)—El Valle, Dominican Republic; (J)—Sarawak, Borneo, Malaysia.

## 2. Experimental

### 2.1. Sampling

The samples subjected to analysis came from a great collection of fossil resins of Günter Krumbiegel, who was a German geologist and palaeontologist [49]. The specimen's characteristics containing the information on localities, botanical sources and geological environments of deposition as well as detailed data on alterations during diagenesis and/or catagenesis are summarized in Table 1. To provide a correlation between the resins NIR-Raman spectra and their geological backgrounds, only specimens that were not subjected to the redeposition or which provenience was known were used for the study. The oldest resins of the Cretaceous age were considered as non-redeposited.

**Table 1.** Detailed characterization of investigated fossil resins.

Sample Label	Age	Botanical Origin	Geological Settings	Samples Description
Ethiopia	late Cretaceous (late Cenomanian) 93–95 Ma [50,51]	Unknown [50]	Resins occur within Debre Libanos Sandstone Unit (DLSU) from the northwestern Plateau [50]. DLSU represents continental, alluvial to fluvial depositional environment. It consists of medium to coarse grained sandstones showing dune-scale trough cross-bedding and horizontal stratifications. The DLSU unit was deposited during the NE–SW-directed extension related to Mesozoic rifting of Gondwana [52]. Those deposits are overlaid by Early-Late Oligocene volcanic rocks (basalts, trachytes, rhyolites).	Black colour, opacity
Russia, Khatanga	lower Cretaceous (Aptian-Albian) 125–100.5 Ma [53]/ upper Cretaceous (Santonian) 85.8 Ma [54,55]	Unknown [54,56]	Resins occur within Begichev Formation (Eastern Taymir) [57]. It consists of lagoon and coastal sediments of alluvial origin (sands) with interbeddings of clays, aleurites and coal horizons [53].	Red to brown colour, transparency
Myanmar (Burma)	upper Cretaceous (Cenomanian?/Turonian?) 93.5 Ma [58]	<i>Araucariaceae</i> / <i>Pinaceae</i> / <i>Cupressaceae</i> [59]	Amber-bearing sediments are clastic sedimentary rocks ranging from fine sandstones to shales. The amber discs lie parallel to the bedding planes of finer sediment [60]. Volcanic event dated on Cenomanian is reflected in the presence of volcanic clasts.	Red to brown colour, transparency
Russia, Sakhalin Island	middle Eocene 43–47 Ma [61]; Paleocene–65.5 Ma [53]	Ancient species of the gymnosperm families <i>Cupressaceae</i> / <i>Taxodiaceae</i> [53]	Quartzite altered at the p-T conditions of catagenesis [53]	Red to brown colour, transparency, shape of flat discs
Mexico, Chiapas	lower Miocene–middle Miocene 22.5–26 Ma [62]	Extinct <i>Hymenaea mexicana</i> [62]	Resins occur within three lithostratigraphic formations: Marine calcareous sandstones and silt with beds of lignite—the Early Miocene Quinta or Simojovel Fm, the Lower Middle Miocene dark-grey shales of the Mazantic Shale, Lower Miocene grey-blue to grey-green sandstones of the Balumtun Fm [62]	Yellow to brown colour, transparency
Dominican Republic (Cordillera Oriental) El Valle	lower Miocene–middle Miocene 15–20 Ma [63]	<i>Hymenaea</i> [64,65]	The Yanigua Formation is the amber-bearing unit of the eastern area of the Dominican Republic. Formation consists of conglomerates, dark clays, laminated sandy clays, lignite and carbonaceous clays and sandstones. These beds contain flattened and irregular inclusions of amber, usually as pockets or lenses ranging from a few millimeters to several centimeters in size, and may also contain fresh to brackish water ostracods and molluscs [64,66]	Yellow to brown colour, transparency, visible strong blue fluorescence
Dominican Republic (Cordillera Septentrional Santiago de los Caballeros)	late Oligocene–early Miocene 20–25 Ma [64,65]	<i>Hymenaea</i> [64,65]	The La Toca Formation is the second amber-bearing unit of the northern part of the Dominican Republic. Its thickness is estimated at ca. 1200 m. There are mainly clastic (conglomerates and sandstones) rocks cutting by thin lignite beds with fragments of carbonized wood. This is probably an accumulation of deposits in different environments from deltaic to deepwater [64,66,67]	Yellow to brown colour, transparency, visible strong blue fluorescence
Borneo, Sarawak, Malaysia	Neogene/ Miocene; middle Miocene 15–17 Ma [55]	<i>Dipterocarpus</i> [55]	During the earliest Middle Miocene volcanic activity increased. Merit Pila amber was formed together within a layer of brown coal in the Nyalau Formation (NF). The unit consists of sandstones, coal layers and conglomerates. These sediments were deposited under humid tropical conditions. Amber was formed in a damp swamp surrounded by mountainous terrain. Deposition occurred in the lake and wetland flooded by sea water [68,69]	Yellow to brown colour, transparency, visible blue fluorescence
Sumatra, Jambi, Indonesia	lower Miocene–middle Miocene 15–23 Ma [70,71]	<i>Dipterocarpaceae</i> family belonging to angiosperms group [70,71]	Resins occur in coal layers (lignite beds) within middle Miocene sediments representing the transgressive depositional system of Talang Akar Formation (TAF). Sediments were uplifted, folded and faulted due to the Pliocene–Pleistocene orogeny associated with volcanic activity [72,73]	Yellow to brown colour, transparency, visible strong blue fluorescence
Sumatra, Palembang, Indonesia	lower Miocene –23 Ma [70,71]	<i>Dipterocarpaceae</i> [70,71]		Yellow to brown colour, very strong blue fluorescence

## 2.2. Analytical Methods

NIR-Raman spectra of the resins were recorded with two different spectrometers, i.e., handheld and benchtop, to verify the results and indicate the most reliable and informative measuring ranges, especially for the portable Raman instrument. The handheld device was Rigaku Progeny ResQ model equipped with a InGaAs detector device. The tests were feasible thanks to the courtesy of Tusnovics Instruments Ltd., Krakow (Poland). Another instrument was a laboratory grade Thermo Fisher Scientific NXR 9650 FT-Raman module, (Thermo Fisher Scientific, Madison, WI, USA). Both spectrometers worked with 1064 nm laser line excitation and the same detector type.

The Rigaku dispersive spectrometer was equipped with Nd:YAG laser of maximum power value of 490 mW. The spectra were recorded in the range of 2000–200  $\text{cm}^{-1}$ . The results were collected from at least three different analytical points on flat clean surfaces of samples. The spectra obtained differed slightly only in signal intensity. In the case of a portable Raman spectrometer, the sample was held in the hand and short scanning time was needed to obtain undisturbed spectra. Therefore, spectra were obtained from 10 scans with the resolution 8–11  $\text{cm}^{-1}$  as a compromise between scanning time and spectrum quality. Laser power was optimized for the samples and no burn and/or carbonization of the samples were observable under the microscope (MOTIC SNZ-168, Xiamen, China). Raman spectra were baseline corrected and normalized for ease of comparison purposes. The normalized procedure was performed with respect to the most intense band in the range (band with maximum  $\sim 1440 \text{ cm}^{-1}$ ). The baseline correction was an automatic function of the portable device.

The Thermo Electron FT-Raman device uses Nd:YVO<sub>4</sub> laser of a maximum power up to 2.5 W, and XT-KBr beam splitter, gold plated mirrors and 180 degrees reflective accessory for samples acquisition. Each spectrum was acquired in the same analytical conditions. 3200 scans were collected and averaged for each spectrum. Such a high number of repetitions is frequently chosen by spectrometrists in the case of weakly scattering samples measured by Fourier Transform Raman spectroscopy. The selected resolution was 4  $\text{cm}^{-1}$  with a spectral range from 3700  $\text{cm}^{-1}$  to 150  $\text{cm}^{-1}$ . The laser power on the sample was optimized and finally set below 300 mW, to avoid thermal effects on the sample.

## 3. Results and Discussion

### 3.1. Comparison between NIR-Raman Portable, Handheld vs. Laboratory Benchtop Device for Fossil Resins Characterization

The quality of the Raman spectra of fossil resins seems to depend on many parameters, i.e., number of scans, laser power, and signal processing. In the case of an organic material, application of the high energy laser used to obtain Raman spectra might result in thermal alteration of the investigated samples. Therefore, a compromise between laser power and several scan repetitions was reached to obtain a reasonable signal-to-noise ratio in the recorded Raman spectra. The collection and superposition of many scans is a very lengthy process and it can be done by laboratory-grade equipment. In portable, handheld, Raman spectrometers, the duration of the measurement is very limited thus the equipment is considered to be less sensitive than lab equipment. Despite these limitations, it was previously shown that the Baltic amber produces very similar NIR-Raman spectra, irrespective of spectrometer type, i.e., portable or lab instrument [33]. In our work, the compatibility of Raman spectra between a lab, and handheld equipment was also quite good; however, in the case of the portable spectrometer, only the most intense signals could be unambiguously assigned as characteristic Raman bands of functional chemical groups. The positions of the strongest peaks were almost identical on spectra collected from both instruments, as well as the bands shapes in this case. In consequence, despite the difference of the spectral resolution between these two devices, it was possible to distinguish the main amber types. However, differences were found in the relative band intensities, especially for  $\sim 1650 \text{ cm}^{-1}$  and  $\sim 1450 \text{ cm}^{-1}$  lines (Figures 2–5). Moreover, the Raman spectra collected from the laboratory instrument was a little bit more detailed, and more reliable especially in the region  $< 800 \text{ cm}^{-1}$ .

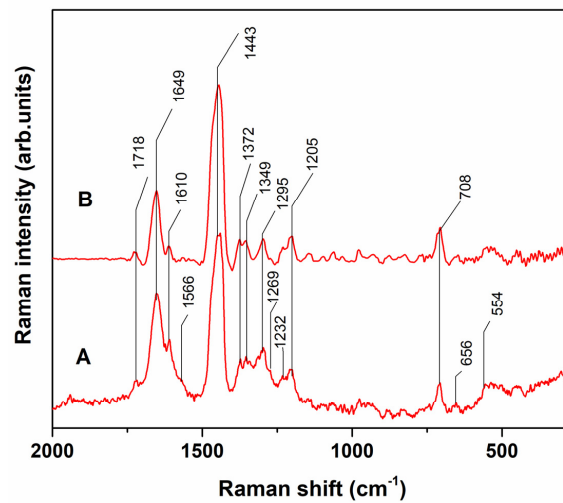


**Figure 2.** Comparison of Raman spectra of fossil resin from Sakhalin (Russia) collected with laboratory (A) and handheld (B) equipment.

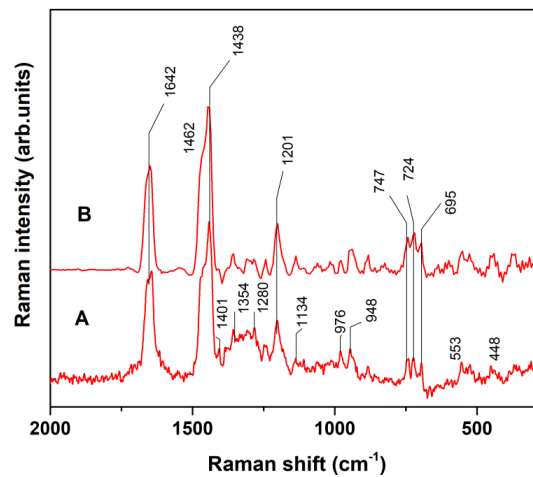


**Figure 3.** Comparison of Raman spectra of fossil resin from Dominican Republic (Santiago de los Caballeros) collected with laboratory (A) and handheld (B) equipment.

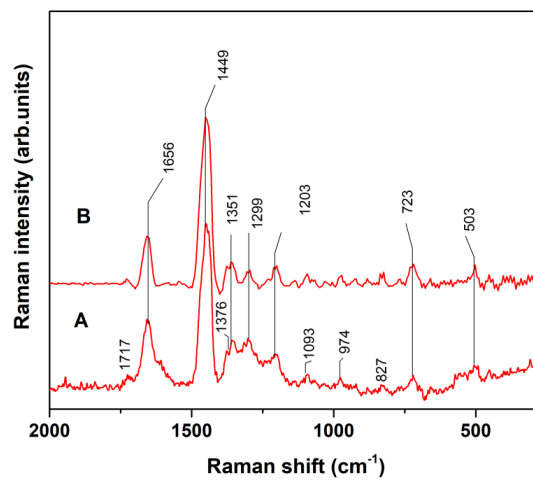


**Figure 4.** Comparison of Raman spectra of fossil resin from Myanmar collected with laboratory (A) and handheld (B) equipment.

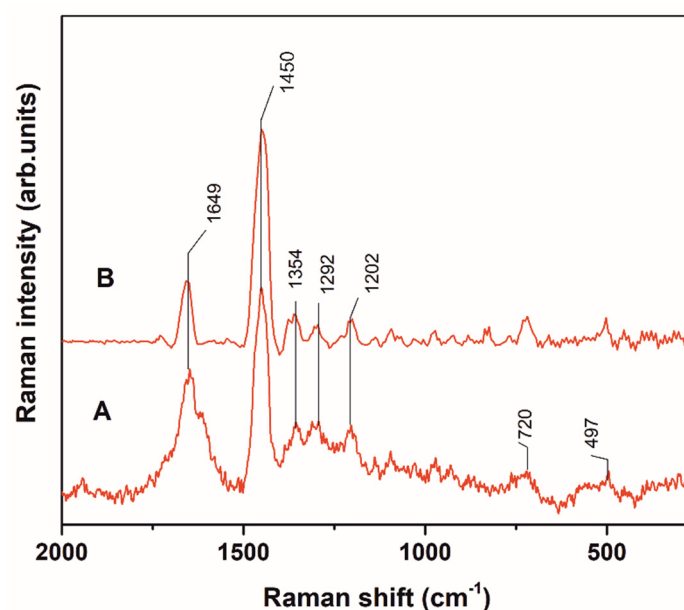


**Figure 5.** Comparison of Raman spectra of resin from Khatanga (Russia) collected with laboratory (A) and handheld (B) equipment.

### 3.2. Fossil Resins Grouping Based on Criteria of Geographical Origin and Botanical Source

The wavenumber positions of the bands in NIR-Raman spectra of the fossil resins collected with a handheld device is listed in Table 2 with their tentative assignments. In general, spectral profiles depend mostly on geographical locations of the samples, their botanical sources as well as maturation grade and geological conditions of their alterations.

The most distinctive Raman spectra were obtained for resins from Sumatra and Borneo Islands. They differed from other resins due to the absence of the peak at  $1200\text{ cm}^{-1}$  that is usually assigned to  $\delta\text{CCH}$  modes of terpenoids [28] or  $\delta\text{COH}$  [23]. Moreover, the extra band at  $800\text{ cm}^{-1}$  was only present in the spectra of resins from Sumatra and Borneo (Figure 6). It could be attributed to aromatic hydrocarbon deformations [27], where its presence would explain the strong luminescence properties of these resins. The Indonesian resins were associated with coal horizons (Table 1), and thus they were probably susceptible to aromatization processes during their fossilization [74]. The presence of the aromatic compounds in the chemical profile of Sumatran fossil resins was confirmed with use of the GC-MS technique. In addition to cyclic compounds from the sesquiterpenoids group, aromatics were present in the form of Cadina-1 (10),6,8-triene ( $\alpha$ -Calamine) and Cadina-1,3,5-triene (L-calamenene). The results are planned to be published in the frame of another paper. On the other hand, specific Raman spectra of Indonesian resins could be explained by their different botanical precursors (*Dipterocarpaceae* family source) as previously concluded by Edwards et al. [19]. The presence of aromatic compounds has also been revealed for Russian resin from Sakhalin Island, which was altered under catagenetic conditions (Table 1). The presence of a band at  $1610\text{ cm}^{-1}$ , which could be attributed to  $\nu(\text{C}=\text{C})$  aromatic [24], suggests that aromatization was a significant part of the maturation process of this resin type. The presence of aromatic compounds in Sakhalin resin has been previously documented due to the GC-MS data by Bechtel et al. [75]. It stays in correlation with the fact that aromatization is one of the most important reactions occurring in organic matter during catagenesis [28].

**Table 2.** NIR-Raman bands ( $\text{cm}^{-1}$ ) for the analysed resins and their tentative assignment.

Ethiopia	Russia (Khatanga)	Myanmar	Russia (Sakhalin Island)	Mexico (Chiapas)	Dominican Republic (El Valle)	Dominican Republic (Santiago de los Caballeros)	Borneo (Sarawak)	Sumatra (Jambi)	Sumatra (Palembang)	Proposed Band Assignment
-	-	-	-	-	371	-	-	-	-	$\delta(\text{CCC})$ [24]
444	-	-	-	445	439	-	-	-	-	unknown
-	497	503	-	-	-	-	-	-	-	$\nu(\text{COC})$ [24]
555	-	-	-	554	-	-	-	-	-	$\delta(\text{CCO})$ [24]
-	-	-	-	-	695	695	-	-	-	$\nu(\text{CC})$ isolated [24]
720	720	723	708	718	720	724	732	731	733	$\nu\text{-C-C}$ [25]
-	-	-	-	-	744	747	-	-	-	$\nu(\text{CC})$ isolated [24]
-	-	-	-	-	-	-	800	799	800	aromatic hydrocarbonsdeformations [27]
1201	1202	1203	1205	1203	1202	1201	-	-	-	$\delta(\text{CCH})$ [24]
1299	1292	1299	1295	1296	-	-	1315	1316	1316	$\delta(\text{CH}_2)$ , $\delta(\text{CH}_3)$ [24]
-	-	-	1349	-	-	-	-	-	1330	$\delta(\text{CH}_2)$ , $\delta(\text{CH}_3)$ [24]
1360	1354	1351	1372	1357	-	-	1360	1360	-	$\delta(\text{CH}_2)$ , $\delta(\text{CH}_3)$ [24]
1443	1450	1449	1443	1442	1442	1462/1438	1449	1442	1442	$\delta(\text{CH}_2)$ , $\delta(\text{CH}_3)$ [24]
-	-	-	1610	-	-	-	-	-	-	$\nu(\text{C=C})$ aromatic [24]
1652	1649	1656	1649	1653	1658	1642	1657	1657	1657	$\nu(\text{C=C})$ non conj. [24]

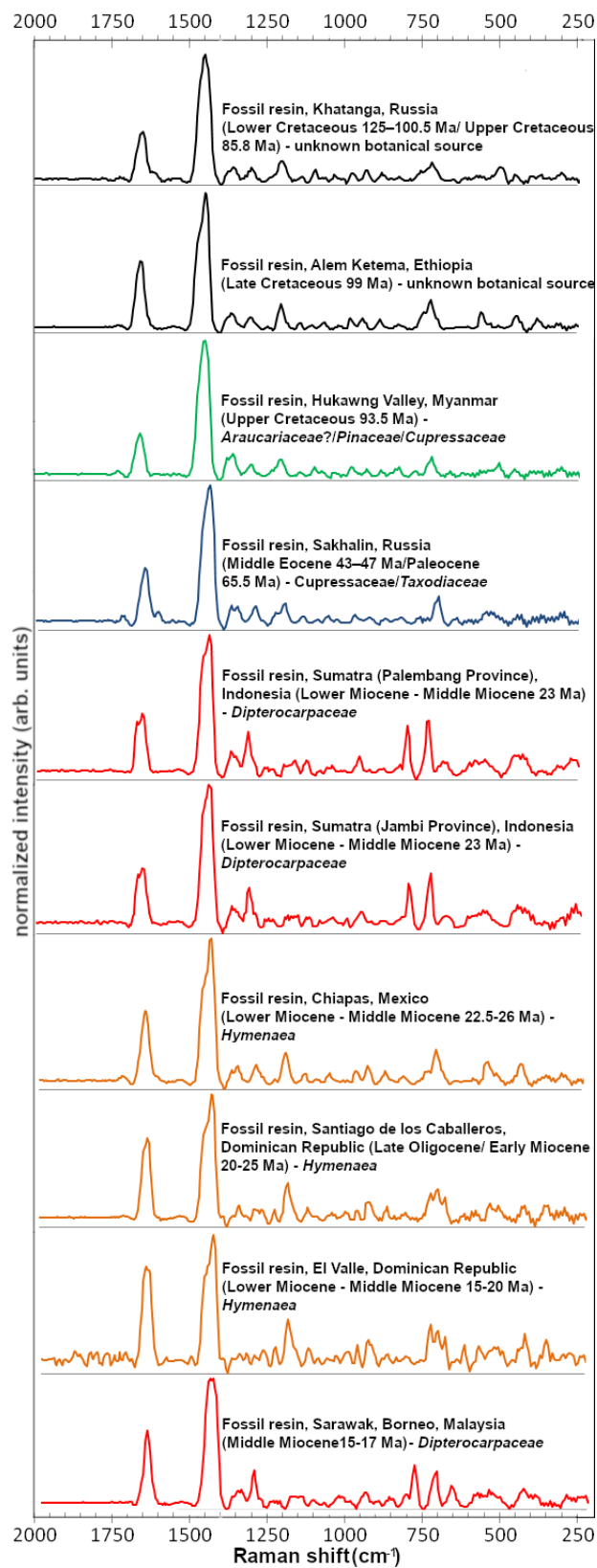


**Figure 6.** Raman spectra of fossil resins, arranged from the oldest to youngest, collected with hand-held equipment. Fossil resins of a similar botanical source have been underlined through the use of specific colour lines.

Despite the similar botanical sources (*Hymenaea*) and age (Miocene), the resins from the Dominican Republic differ from Mexican specimens (Figure 6) mainly due to the presence of a characteristic triplet found at 747, 724 and 695  $\text{cm}^{-1}$  maxima (Figures 3 and 6). These bands have been previously observed by Brody et al. [24] with the use of a laboratory, benchtop device. Now, for the first time, their presence is also confirmed by means of the portable, handheld instrument. These spectral differences might reflect variations of resins source plants at the species level. Likely, the Mexican resins were produced by extinct *H. Mexicana* [76] and/or *H. allendis* species [77], while Dominican species were probably formed from exudates of *H. verrucos* [78] as evidenced from FT-IR and  $^{13}\text{C}$  NMR spectroscopic methods [78]. In turn, Mexican and Ethiopian resins exhibit a great similarity in their NIR-Raman spectra characteristics. Specimens from Ethiopia, that have been already discovered [50], remain one of the less known fossil resins of Cretaceous [50] or Miocene age [79]. The genus *Hymenaea* has been proposed as a botanical source of Ethiopian resins [79] based on the organic inclusions data as well as chemical composition revealed by the use of solid phase microextraction gas chromatography-mass spectrometry [80]. On the basis of Raman spectroscopy, the similarity between Ethiopian and Mexican fossil resins could be found. As a result, the origin of Ethiopian resin from *Hymenaea* could be concluded.

Although spectra obtained from the portable Raman spectrometer allowed for the observation of only the most intense bands, a preliminary identification of the botanical source and fossil resins grouping seemed to still be possible with the application of this technique. Such portable equipment might be therefore used for preliminary screening of the material and selection of more advanced techniques with the use of laboratory spectrometers or other instrumental methods (i.e., GC-MS, thermal analysis).

### 3.3. Fossil Resins Grouping Based on Age/Maturation Grade Criteria

The process of fossil resin maturation is initiated at the time of the exudation under hypergenic conditions influenced by sun heating, and the temperature of the surrounding environment [7]. Further alteration of fossil resins could be very slow and gradual; however, it might also be accelerated by forest fires or geological events, e.g., volcanic activity, an increase in temperature due to burial conditions or the development of orogens. During fossilization, the resins have undergone many chemical processes, such as aromatization, catenation, compound cross-linking and dehydrogenation induced by various environmental and geological conditions [7,28].

Along with the maturation process, penta- and hexacyclic rings in terpenoids undergo aromatization. The degradation of fossil resins results in loss of  $\nu(\text{C}=\text{C})$  non-aromatic unsaturation, which is marked by the lower intensity of the band at 1640  $\text{cm}^{-1}$  compared with 1440  $\text{cm}^{-1}$  [25]. Thus, the intensity ratio bands I(1640/1440) has been proposed as an indicator of the maturation degree of organic matter, especially for fossil resins [25]. Although the assignment of these two bands is still disputable, one may assume, based on previous studies, that the 1440  $\text{cm}^{-1}$  band is characteristic of vibration in  $\text{CH}_2$  groups, and the 1640  $\text{cm}^{-1}$  band is due to  $\text{C}=\text{C}$  stretching vibration [25]. Additionally, the presence of a broad band at  $\sim 714 \text{ cm}^{-1}$  was previously interpreted as an indicator of the resin's maturation grade [28].

The application of an I(1640/1440) indicator for assessment of fossil resins age has been frequently carried out despite the fact that the maturation of fossil resins is not only a function of time but is strongly dependent on their burial history [e.g., 25,28]. The botanical source of the resins and their primary environment also play an important role in the maturation process pathways [28]. The presented results confirm that assessment of resin age based on the height ratio of 1640/1440  $\text{cm}^{-1}$  is very difficult or even impossible, as any correlation between the resins characteristic and their calculated height ratio of 1640/1440  $\text{cm}^{-1}$  was found in our research (Figure 6, Table 3). However, the maturation grade of the resins could be revealed when their geological background is taken into consideration. It was concluded that the temperature conditions of the resin burial had the greatest influence on fossilization processes, while volcanism seemed to be the most important geological factor that determined not only the production of resins [81] but also their alteration rate affected by

heating. Fossil resins that underwent alteration controlled by the volcanic heating showed a lower height ratio of 1640/1440  $\text{cm}^{-1}$  than expected from their geological age (i.e., resins from Sumatra and Myanmar, vide Table 1). Probably thermal or/and hydrothermal processes associated with the volcanic activity may cause partial oxidation or breaking of double bonds in compounds present in these resins. The pressure-temperature (p-T) conditions of diagenesis also influence the polymerization degree of the resins. The relatively young resin from Sakhalin Island (Russia), which showed a height ratio of 1640/1440  $\text{cm}^{-1}$  close to the Cretaceous resins from Myanmar and Khatanga (Russia) (Figures 2–6), occurring in quartzite layers (Table 1), was likely altered due to the catagenic or oxidation processes, which, in turn, diminished the number of unsaturated bonds. Those results stay in correlation with thermal analysis [82] performed on Sumatran and Russian specimens, which confirmed that those resins were subjected to elevated p-T conditions. Another unexpected result was obtained for Ethiopian fossil resins. Their height ratios of 1640/1440  $\text{cm}^{-1}$ , as being indicative for low polymerization degree, might confirm younger than the Cretaceous age of these specimens [51,80]; however, geological data also suggest low temperature conditions of their diagenesis.

**Table 3.** Comparison of bands height ratios I(1640/1440) calculated on the basis of portable spectrometer results.

Age	Sample label	Height Ratio of 1640/1440 $\text{cm}^{-1}$
Cretaceous	Ethiopia	0.51 ± 0.01
Cretaceous	Russia (Khatanga)	0.40 ± 0.06
Cretaceous	Myanmar	0.33 ± 0.02
Eocene	Russia (Sakhalin Island)	0.36 ± 0.01
Miocene	Mexico (Chiapas)	0.52 ± 0.01
Miocene	Dominican Republic (El Valle)	0.79 ± 0.02
Miocene	Dominican Republic (Santiago de los Caballeros)	0.66 ± 0.12
Miocene	Borneo (Sarawak)	0.60 ± 0.03
Miocene	Sumatra (Jambi)	0.44 ± 0.06
Miocene	Sumatra (Palembang)	0.46 ± 0.02

Further problems with the application of the height ratio of 1640/1440  $\text{cm}^{-1}$  for proper assessment of resins age/maturation grade arises from differences in bands intensity between handheld measurements and a laboratory grade Raman device, which might be explained by different spectral resolutions. As always in the case of the preparation of analytical methods, one needs to have very well-defined rules in order to prepare reproducible spectra. Otherwise, investigators would have a problem with interpretation and comparison of spectra reported in literature.

To sum up, the height ratio of 1640/1440  $\text{cm}^{-1}$  cannot be used as a general approach to resins dating, however, it still might have application for comparison of the age of samples altered under the same or similar pressure-temperature conditions in host deposits and from the same kind of botanical sources. The combination of this index with other, independent analytical techniques might provide new indicators of resins age irrespective of their provenance and geological history. FT-Raman spectroscopy coupled with a chemometric analysis has been already performed by Peris-Diaz et al. [37] presenting quite a good result of PLS (partial least squares classification analysis) according to resins age (Cretaceous and Cenozoic periods). Beltran et al. [36] performed Raman and IR spectroscopic analysis of resin specimens coming from *Pinus*, and pointed out characteristic compounds of fresh and aged samples. However, further effort should be done to find indicators of fossil resins polymerization degree with respect to their burial conditions, not the ageing itself. Moreover, the height ratio of the bands with maxima near 1640  $\text{cm}^{-1}$  and 1440  $\text{cm}^{-1}$  cannot be considered as an indicator of resins maturation grade until restrictive rules regarding data collection and processing are defined.

#### 4. Conclusions

1. The Raman spectra of fossil resins, coming from various worldwide localities, and differing in age, botanical source, history of evolution and geological background, obtained with handheld, portable NIR-Raman spectrometer were very similar to these collected with a more advanced, benchtop Raman instrument. The only differences were found in the spectral region  $<800\text{ cm}^{-1}$ , and locally in the intensities of some Raman bands.
2. The differentiation of fossil resins of the same age and botanical source, coming from various geographical localities with Near infrared Raman spectroscopy is possible for samples coming from the Dominican Republic and Mexico (Miocene, *Hymenae*), but out of the question for specimens from Sumatra and Borneo (Miocene, *Dipterocarpaceae*). On the other hand, similar spectral features obtained for specimens of various ages and geographical localities may result from the same botanical source, as noted for resins coming from Ethiopia and Mexico. Hence, it was found that spectral features which reflect the chemical composition of fossil resins seem to depend mainly on their botanical source. Other factors affecting the features of Raman spectra are strongly connected with the alteration and maturation processes of the fossil resins.
3. There was no direct correlation between the height ratio of  $1640/1440\text{ cm}^{-1}$ , which is commonly regarded as indicator of maturation grade, and fossil resins age. Interestingly, specimens of the same age (e.g., Dominican and Sumatran resins both of Miocene age) showed a different  $1640/1440\text{ cm}^{-1}$  height ratio index, caused probably by the alterations under various temperature and pressure conditions. Hence, it was concluded, this  $1640/1440\text{ cm}^{-1}$  height ratio index can provide additional data on geological events proceeding from the time of exudation through transportation, deposition in sedimentary basin to exhumation and re-exposure to hypergenic conditions, and thus will reflect the evolutionary history of resins.

**Author Contributions:** B.N., M.M.-S., M.D.-S., L.N.-N. and P.D. designed the experiments, interpreted the data and wrote the paper. M.M.-S., P.S. and P.D. performed the experiments and prepared figures and photographs. G.Ž. substantively revised the first version of the manuscript. All authors have read and agreed to the published version of the manuscript.

**Funding:** The work was financially supported by AGH University of Science and Technology (Krakow Poland), grant No 16.16.140.315 and the Polish Geological Institute-National Research Institute, research project No. 61.9012.1908.00.0.

**Acknowledgments:** Anselm Krumbiegel is acknowledged for providing specimens of fossil resin for the research. Rastislav Milovsky is acknowledged for providing GC-MS data for the Sumatran resin. We thank the anonymous reviewers for their constructive comments and the editor for handling the paper.

**Conflicts of Interest:** The authors declare no conflicts of interest.

#### References

1. Bartenev, G.M. *Physics and Mechanics of Polymers*; Chemistry Press: Moscow, Russia, 1983.
2. Grimalt, J.O.; Simoneit, B.R.T.; Hatcher, P.G.; Nissenbaum, A. The molecular composition of ambers. *Org. Geochem.* **1988**, *13*, 677–690. [[CrossRef](#)]
3. Gold, D.; Hazen, B.; Miller, W.G. Colloidal and polymeric nature of fossil amber. *Org. Geochem.* **1999**, *30*, 971–983. [[CrossRef](#)]
4. Colchester, D.M.; Webb, G.; Emseis, P. Amber-like fossil resin from north Queensland, Australia. *Aust. Gemm.* **2006**, *22*, 378–385.
5. Menor-Salván, C.; Simoneit, B.R.; Ruiz-Bermejo, M.; Alonso, J. The molecular composition of Cretaceous ambers: Identification and chemosystematic relevance of 1,6-dimethyl-5-alkyltetralins and related bisnorlabdane biomarkers. *Org. Geochem.* **2016**, *93*, 7–21. [[CrossRef](#)]
6. Roghi, G.; Ragazzi, E.; Gianolla, P. Triassic amber of the southern Alps (Italy). *Palaios* **2006**, *21*, 143–154. [[CrossRef](#)]
7. Ragazzi, E.; Alexander, R.S. (Eds.) Amber. In *Encyclopedia of Geobiology*; Springer: Dordrecht, The Netherlands, 2011; pp. 24–36.

8. Beck, C.; Wilbur, E.; Meret, S.; Kossove, D.; Kermani, K. The infrared spectra of amber and the identification of Baltic amber. *Archaeometry* **1965**, *8*, 96–109. [[CrossRef](#)]
9. Gough, L.J.; Mills, J.S. The composition of succinite (Baltic Amber). *Nature* **1972**, *239*, 527–528. [[CrossRef](#)]
10. Mills, J.S.; White, R.; Gough, L.J. The chemical composition of Baltic amber. *Chem. Geol.* **1984**, *47*, 15–39. [[CrossRef](#)]
11. Mosini, V.; Samperi, R. Correlations between baltic amber and *Pinus resins*. *Phytochemistry* **1985**, *24*, 859–861. [[CrossRef](#)]
12. Pakutinskiene, I.; Kiuberis, J.; Bezdicka, P.; Senvaitiene, J.; Kareiva, A. Analytical characterization of Baltic amber by FTIR, XRD and SEM. *Can. J. Anal. Sci. Spectrosc.* **2007**, *52*, 287–293.
13. Wolfe, A.P.; Tappert, R.; Muehlenbachs, K.; Boudreau, M.; McKellar, R.C.; Basinger, J.F.; Garrett, A. A new proposal concerning the botanical origin of Baltic amber. *Proc. R. Soc. B Biol. Sci.* **2009**, *276*, 3403–3412. [[CrossRef](#)] [[PubMed](#)]
14. Galletti, G.C.; Mazzeo, R. Pyrolysis/gas chromatography/mass spectrometry and Fourier-transform infrared spectroscopy of amber. *Rapid Commun. Mass Spectrom.* **1993**, *7*, 646–650. [[CrossRef](#)]
15. Guiliano, M.; Asia, L.; Onoratini, G.; Mille, G. Applications of diamond crystal ATR FTIR spectroscopy to the characterization of ambers. *Spectrochim. Acta Part A Mol. Biomol. Spectrosc.* **2007**, *67*, 1407–1411. [[CrossRef](#)] [[PubMed](#)]
16. Golubev, Y.A.; Martirosyan, O.V. The structure of the natural fossil resins of North Eurasia according to IR-spectroscopy and microscopic data. *Phys. Chem. Miner.* **2012**, *39*, 247–258. [[CrossRef](#)]
17. Drzewicz, P.; Natkaniec-Nowak, L.; Czaplá, D. Analytical approaches for studies of fossil resins. *TrAC Trends Anal. Chem.* **2016**, *85*, 75–84. [[CrossRef](#)]
18. Kosmowska-Ceranowicz, B.; Vávra, N. *Infrared Spectra of Fossil Resins, Subfossil Resins and Selected Imitation of Amber*; Polish Academy of Science Museum of Earth: Warsaw, Poland, 2015.
19. Edwards, H.G.; Farwell, D.W.; Villar, S.E.J. Raman microspectroscopic studies of amber resins with insect inclusions. *Spectrochim. Acta Part A Mol. Biomol. Spectrosc.* **2007**, *68*, 1089–1095. [[CrossRef](#)]
20. Garty, J.; Giele, C.; Krumbein, W.E. On the occurrence of pyrite in a lichen-like inclusion in Eocene amber (Baltic). *Palaeogeogr. Palaeoclimatol. Palaeoecol.* **1982**, *39*, 139–147. [[CrossRef](#)]
21. Grimaldi, D.; Bonwich, E.; Delannoy, M.; Doberstein, S. Electron Microscopic Studies of Mummified Tissues in Amber Fossils. *Am. Mus. Novit.* **1994**, *3097*, 1–31.
22. Edwards, H.G.M.; Farewell, D.W. Fourier transform-Raman spectroscopy of amber. *Spectrochim. Acta Part A Mol. Biomol. Spectrosc.* **1995**, *52*, 1119–1125. [[CrossRef](#)]
23. Moreno, Y.M.; Christensen, D.H.; Nielsen, O.F. A NIR-FT-Raman spectroscopic study of amber. *Asian J. Spectrosc.* **2000**, *4*, 49–56.
24. Brody, R.H.; Edwards, H.G.M.; Pollard, A.M. A study of amber and copal samples using FT-Raman spectroscopy. *Spectrochim. Acta Part A Mol. Biomol. Spectrosc.* **2001**, *57*, 1325–1338. [[CrossRef](#)]
25. Winkler, W.A.; Kirchner, E.C.; Asenbaum, A.; Musso, M. A Raman spectroscopic approach to the maturation process of fossil resins. *J. Raman Spectrosc.* **2001**, *32*, 59–63. [[CrossRef](#)]
26. Winkler, W.; Musso, M.; Kirchner, E.C. Fourier transform Raman spectroscopic data on the fossil resin siegburgite. *J. Raman Spectrosc.* **2003**, *34*, 157–162. [[CrossRef](#)]
27. Vandenabeele, P.; Grimaldi, D.M.; Edwards, H.G.M.; Moens, L. Raman spectroscopy of different types of Mexican copal resins. *Spectrochim. Acta Part A Mol. Biomol. Spectrosc.* **2003**, *59*, 2221–2229. [[CrossRef](#)]
28. Jehlička, J.; Villar, S.E.J.; Edwards, H.G.M. Fourier transform Raman spectra of Czech and Moravian fossil resins from freshwater sediments. *J. Raman Spectrosc.* **2004**, *35*, 761–767. [[CrossRef](#)]
29. Shashoua, Y.; Degn Berthelsen, M.B.L.; Nielsen, O.F. Raman and ATR-FTIR spectroscopies applied to the conservation of archaeological Baltic amber. *J. Raman Spectrosc.* **2006**, *37*, 1221–1227. [[CrossRef](#)]
30. Jehlička, J.; Edwards, H.G.M. Raman spectroscopy as a tool for the non-destructive identification of organic minerals in the geological record. *Org. Geochem.* **2008**, *39*, 371–386. [[CrossRef](#)]
31. Jehlička, J.; Vitek, P.; Edwards, H.G.M.; Heagraves, M.; Čapoun, T. Application of portable Raman instruments for fast and non-destructive detection of minerals on outcrops. *Spectrochim. Acta Part A Mol. Biomol. Spectrosc.* **2009**, *73*, 410–419. [[CrossRef](#)]
32. Jehlička, J.; Vitek, P.; Edwards, H.G.M.; Hargreaves, M.; Čapoun, T. Rapid outdoor non-destructive detection of organic minerals using a portable Raman spectrometer. *J. Raman Spectrosc.* **2009**, *40*, 1645–1651. [[CrossRef](#)]

33. Vítek, P.; Ali, E.M.A.; Edwards, H.G.M.; Jehlička, J.; Cox, R.; Page, K. Evaluation of portable Raman spectrometer with 1064nm excitation for geological and forensic applications. *Spectrochim. Acta Part A Mol. Biomol. Spectrosc.* **2012**, *86*, 320–327. [[CrossRef](#)]
34. Rao, Z.; Dong, K.; Yang, X.; Lin, J.; Cui, X.; Zhou, R.; Deng, Q. Natural amber, copal resin and colophony investigated by UV-VIS, infrared and Raman spectrum. *Sci. China Phys. Mech. Astron.* **2013**, *56*, 1598–1602. [[CrossRef](#)]
35. Havelcová, M.; Machovič, V.; Linhartová, M.; Lapčák, L.; Přichystal, A.; Dvořák, Z. Vibrational spectroscopy with chromatographic methods in molecular analyses of Moravian amber samples (Czech Republic). *Microchem. J.* **2016**, *128*, 153–160. [[CrossRef](#)]
36. Beltran, V.; Salvadó, N.; Butí, S.; Cinque, G.; Pradell, T. Markers, reactions, and interactions during the aging of pinus resin assessed by Raman spectroscopy. *J. Nat. Prod.* **2017**, *80*, 854–863. [[CrossRef](#)] [[PubMed](#)]
37. Peris-Díaz, M.D.; Łydzba-Kopczyńska, B.; Sentandreu, E. Raman spectroscopy coupled to chemometrics to discriminate provenance and geological age of amber. *J. Raman Spectrosc.* **2018**, *49*, 842–851. [[CrossRef](#)]
38. Anderson, K.B.; Winans, R.E. Nature and fate of natural resins in the geosphere. I. Evaluation of pyrolysis-gas chromatography mass spectrometry for the analysis of natural resins and resinites. *Anal. Chem.* **1991**, *63*, 2901–2908. [[CrossRef](#)]
39. Tonidandel, L.; Ragazzi, E.; Traldi, P. Mass spectrometry in the characterization of ambers. II. Free succinic acid in fossil resins of different origin. *Rapid Commun. Mass Spectrom.* **2009**, *23*, 403–408. [[CrossRef](#)] [[PubMed](#)]
40. Lambert, J.B.; Frye, J.S.; Poinar, G.O. Amber from the Dominican Republic: Analysis by nuclear magnetic resonance spectroscopy. *Archaeometry* **1985**, *27*, 43–51. [[CrossRef](#)]
41. Lambert, J.B.; Johnson, S.C.; Poinar, G.O., Jr. Resin from Africa and South America: Criteria for distinguishing between fossilized and recent resin based on NMR spectroscopy. *ACS Symp. Ser.* **1995**, *617*, 193–202.
42. Lambert, J.B.; Levy, A.J.; Santiago-Blay, J.A.; Wu, Y. Nuclear magnetic resonance characterization of Indonesian amber. *Life Excit. Biol.* **2013**, *1*, 136–155. [[CrossRef](#)]
43. Ragazzi, E.; Roghi, G.; Giaretta, A.; Gianolla, P. Classification of amber based on thermal analysis. *Thermochem. Acta* **2003**, *404*, 43–54. [[CrossRef](#)]
44. Zhao, J.; Ragazzi, E.; McKenna, G.B. Something about amber: Fictive temperature and glass transition temperature of extremely old glasses from copal to Triassic amber. *Polymer* **2013**, *54*, 7041–7047. [[CrossRef](#)]
45. Pagacz, J.; Stach, P.; Natkaniec-Nowak, L.; Naglik, B.; Drzewicz, P. Preliminary thermal characterization of natural resins from different botanical sources and geological environments. *J. Therm. Anal. Calorim.* **2019**, *138*, 4279–4288. [[CrossRef](#)]
46. Matuszewska, A.; Gołąb, A. Próba wykorzystania parametru mikrotwardośći żywic kopalnych i sztucznych jako cechy klasyfikacyjnej (An attempt at using the parameter of the microhardness of fossil and artificial resins as a classification feature). *Bursztynisko* **2008**, *31*, 56–61. (In Polish)
47. Stach, P.; Martinkutė, G.; Šinkūnas, P.; Natkaniec-Nowak, L.; Drzewicz, P.; Naglik, B.; Bogdasarov, M. An attempt to correlate the physical properties of fossil and subfossil resins with their age and geographic location. *J. Polym. Eng.* **2019**, *39*, 716–728. [[CrossRef](#)]
48. Marshall, C.P.; Edwards, H.G.; Jehlička, J. Understanding the application of Raman spectroscopy to the detection of traces of life. *Astrobiology* **2010**, *10*, 229–243. [[CrossRef](#)] [[PubMed](#)]
49. Kosmowska-Ceranowicz, B. *Amber Researcher Günter Krumbiegel and His Contacts with Poland*; Amberif: Gdańsk, Poland, 2015; pp. 5–7.
50. Schmidt, A.R.; Perrichot, V.; Svojtka, M.; Anderson, K.B.; Belete, K.H.; Bussert, R.; Dörfelt, H.; Jancke, S.; Mohr, B.; Mohrmann, E.; et al. Cretaceous African life captured in amber. *Proc. Natl. Acad. Sci. USA* **2010**, *107*, 7329–7334. [[CrossRef](#)] [[PubMed](#)]
51. Coty, D.; Lebon, M.; Nel, A. When phylogeny meets geology and chemistry: Doubts on the dating of Ethiopian amber. In *Annales de la Société entomologique de France (NS)*; Taylor & Francis: Abingdon, UK, 2016; Volume 52, pp. 161–166.
52. Gani, N.; Abdelsalam, M.G.; Gera, S.; Gani, M.R. Stratigraphic and structural evolution of the Blue Nile Basin, northwestern Ethiopian plateau. *Geol. J.* **2009**, *44*, 30–56. [[CrossRef](#)]
53. Bogdasarow, M.A. *Amber and Others Fossil Resins of Eurasia*; Brest State University AS. Pushkin: Brest, France, 2010; 263p. (In Russian)
54. Remm, H. Midges (Diptera, Ceratopogonidae) from the Upper Cretaceous fossil resins of the Khatanga depression. *Paleontologitsekiy Zhurnal* **1976**, *3*, 107–116.

55. Kosmowska-Ceranowicz, B. *Bursztyn w Polsce i na Świecie (Amber in Poland and in the World)*, 2nd ed.; Wydawnictwo Uniwersytetu Warszawskiego: Warsaw, Poland, 2017; 310p.
56. Poinar, G.O. *Life in Amber*; Stanford University Press: California, CA, USA, 1992.
57. Azar, D.; Adaymeh, C.; Jreich, N. Paleopsychoda zherikhini, a new Cretaceous species of moth flies from Taimyr amber (Diptera: Psychodidae: Psychodinae). *Afr. Invertebr.* **2007**, *48*, 163–168.
58. Grimaldi, D.A.; Engel, M.S.; Nascimbene, P.C. Fossiliferous Cretaceous amber from Myanmar (Burma): Its rediscovery, biotic diversity, and paleontological significance. *Am. Mus. Novit.* **2002**, *2002*, 1–71. [[CrossRef](#)]
59. Shi, G.; Grimaldi, D.A.; Harlow, G.E.; Wang, J.; Wang, J.; Yang, M.; Lei, W.; Li, Q.; Li, X. Age constraint on Burmese amber based on U–Pb dating of zircons. *Cretac. Res.* **2012**, *37*, 155–163. [[CrossRef](#)]
60. Cruickshank, R.D.; Ko, K. Geology of an amber locality in the Hukawng Valley, northern Myanmar. *J. Asian Earth Sci.* **2003**, *21*, 441–455. [[CrossRef](#)]
61. Radchenko, A.G.; Perkowsky, E.E. The ant *Aphaenogaster dluskyana* sp. nov. (Hymenoptera, Formicidae) from the Sakhalin amber—The earliest described species of an extant genus of Myrmicinae. *Paleontol. J.* **2016**, *50*, 936–946. [[CrossRef](#)]
62. Kraemer, M.S. Mexican amber. In *Biodiversity of Fossils in Amber from the Major World Deposits*; Siri Scientific Press: Manchester, UK, 2010; pp. 42–56.
63. Langenheim, J.H. *Plant Resins: Chemistry, Evolution, Ecology, and Ethnobotany*; Timber Press: Portland, OR, US, 2003.
64. Iturralde-Vinent, M.A.; MacPhee, R.D.E. Age and paleogeographical origin of Dominican amber. *Science* **1996**, *273*, 1250–1252. [[CrossRef](#)]
65. Poinar, J. Palaeoecological perspectives in Dominican amber. *Ann. Soc. Entomol. Fr.* **2010**, *46*, 23–52. [[CrossRef](#)]
66. Iturralde-Vinent, M.A. Geology of the amber-bearing deposits of the Greater Antilles. *Caribb. J. Sci.* **2001**, *37*, 141–167.
67. Bachmann, R. *The Caribbean Plate and the Question of Its Formation*; Institute of Geology, University of Mining and Technology, Department of Tectonophysics: Freiberg, Germany, 2001.
68. Liechti, P.; Roe, F.W.; Haile, N.S. *The Geology of Sarawak, Brunei and the Western Part of North Borneo*; Geological Survey Dept: British Territories in Borneo, Borneo, 1960.
69. Hall, R.; van Hattum, M.W.; Spakman, W. Impact of India–Asia collision on SE Asia: The record in Borneo. *Tectonophysics* **2008**, *451*, 366–389. [[CrossRef](#)]
70. Ngô-Muller, V.; Garrouste, R.; Pouillon, J.M.; Christophersen, V.; Christophersen, A.; Nel, A. The first representative of the fly genus *Trentepohlia* subgenus *Mongoma* in amber from the Miocene of Sumatra (Diptera: Limoniidae). *Historical Biology* **2019**, 1–4.
71. Brackman, W.; Spaargaren, K.; Van Dongen, J.P.C.M.; Couperus, P.A.; Bakker, F. Origin and structure of the fossil resin from an Indonesian Miocene coal. *Geochim. Cosmochim. Acta.* **1984**, *48*, 2483–2487. [[CrossRef](#)]
72. Barber, A.J.; Crow, M.J.; Milsom, J.S. (Eds.) *Sumatra: Geology, Resources and Tectonic Evolution*; Geological Society of London: London, UK, 2005.
73. Adiwidjaja, P.; De Coster, G.L. Pre-Tertiary paleotopography and related sedimentation in South Sumatra. In *Proceedings of the Annual Convention—Indonesian Petroleum Association 2*; AAPG: Okla, OK, USA, 1973; pp. 89–103.
74. Naglik, B.; Kosmowska-Ceranowicz, B.; Natkaniec-Nowak, L.; Drzewicz, P.; Dumańska-Słowik, M.; Matusik, J.; Wagner, M.; Milovsky, R.; Stach, P.; Szyszka, A. Fossilization History of Fossil Resin from Jambi Province (Sumatra, Indonesia) Based on Physico-Chemical Studies. *Minerals* **2018**, *8*, 95–107. [[CrossRef](#)]
75. Bechtel, A.; Chekryzhov, I.Y.; Nechaev, V.P.; Kononov, V.V. Hydrocarbon composition of Russian amber from the Voznovo lignite deposit and Sakhalin Island. *Int. J. Coal Geol.* **2016**, *167*, 176–183. [[CrossRef](#)]
76. Poinar, G., Jr.; Brown, A.E. *Hymenaea mexicana* sp. nov. (Leguminosae: Caesalpinioideae) from Mexican amber indicates Old World connections. *Bot. J. Linn. Soc* **2002**, *139*, 125–132. [[CrossRef](#)]
77. Calvillo-Canadell, L.; Cevallos-Ferriz, S.; Rico-Arce, L. Miocene *Hymenaea* flowers preserved in amber from Simojovel de Allende, Chiapas, Mexico. *Rev. Palaeobot. Palynol.* **2010**, *160*, 126–134. [[CrossRef](#)]
78. Cunningham, A.; Gay, I.D.; Oehlschlager, A.C.; Langenheim, J.H. <sup>13</sup>C NMR and IR analyses of structure, aging and botanical origin of Dominican and Mexican ambers. *Phytochemistry* **1983**, *22*, 965–968. [[CrossRef](#)]

79. Perrichot, V.; Boudinot, B.; Cole, J.; Delhaye-Prat, V.; Esnault, J. African fossiliferous amber: A review. In Proceedings of the 7th International Conference on Fossil Insects, Arthropods and Amber, Edinburgh, UK, 26 April–1 May 2016.
80. McCoy, V.E.; Boom, A.; Kraemer, M.M.S.; Gabbott, S.E. The chemistry of American and African amber, copal and resin from the genus *Hymenaea*. *Org. Geochem.* **2017**, *113*, 43–54. [[CrossRef](#)]
81. Kosmowska-Ceranowicz, B.; Sachanbiński, M.; Łydzba-Kopczyńska, B. Analytical characterization of “Indonesian amber” deposits: Evidence of formation from volcanic activity. *Baltica* **2017**, *30*, 55–60. [[CrossRef](#)]
82. Pagacz, J.; Naglik, B.; Stach, P.; Drzewicz, P.; Natkaniec-Nowak, L. Maturation process of natural resins recorded in their thermal properties. *J. Mater. Sci.* **2020**, *55*, 4504–4523. [[CrossRef](#)]



© 2020 by the authors. Licensee MDPI, Basel, Switzerland. This article is an open access article distributed under the terms and conditions of the Creative Commons Attribution (CC BY) license (<http://creativecommons.org/licenses/by/4.0/>).